28 Jun 2022

Ultrasmall Nanodiamonds: Perspectives and Questions

Shery L.Y. Chang

Philipp Reineck

Anke Krueger

Vadym Mochalin
Missouri University of Science and Technology, mochalinv@mst.edu

Recommended Citation

S. L. Chang et al., "Ultrasmall Nanodiamonds: Perspectives and Questions," *ACS nano*, vol. 16, no. 6, pp. 8513 - 8524, American Chemical Society, Jun 2022.
The definitive version is available at https://doi.org/10.1021/acsnano.2c00197

ACS NANO

www.acsnano.org

PERSPECTIVE

Ultrasmall Nanodiamonds: Perspectives and Questions

Shery L. Y. Chang,* Philipp Reineck,* Anke Krueger,* and Vadym N. Mochalin*

Cite This: *ACS Nano* 2022, 16, 8513–8524

Read Online

ACCESS | Metrics & More | Article Recommendations

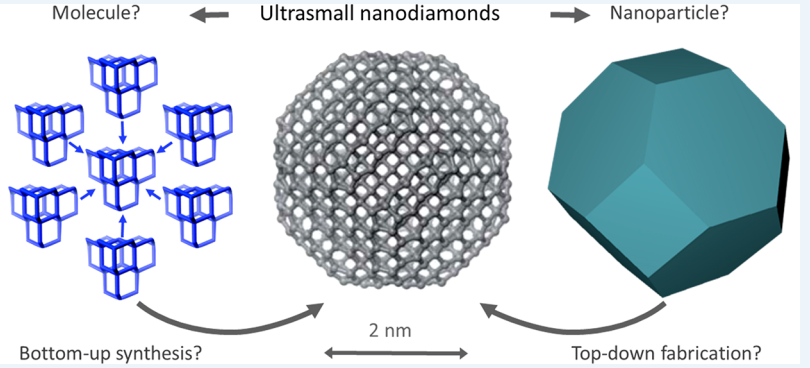

ABSTRACT: **Nanodiamonds are at the heart of a plethora of emerging applications in areas ranging from nanocomposites and tribology to nanomedicine and quantum sensing. The development of alternative synthesis methods, a better understanding, and the availability of ultrasmall nanodiamonds of less than 3 nm size with a precisely engineered composition, including the particle surface and atomic defects in the diamond crystal lattice, would mark a leap forward for many existing and future applications. Yet today, we are unable to accurately control nanodiamond composition at the atomic scale, nor can we reliably create and isolate particles in this size range. In this perspective, we discuss recent advances, challenges, and opportunities in the synthesis, characterization, and application of ultrasmall nanodiamonds. We particularly focus on the advantages of bottom-up synthesis of these particles and critically assess the physicochemical properties of ultrasmall nanodiamonds, which significantly differ from those of larger particles and bulk diamond.**

KEYWORDS: *nanodiamond, diamond, synthesis, characterization*

According to IUPAC,[1] ISO,[2] and ASTM[3] definitions of nanoparticles, nanodiamond (ND) particles can be defined as diamond particles of any shape whose size in all dimensions is between 1 and 100 nm. Historically, the first NDs were produced by detonation synthesis invented in the early 1960s in the former USSR.[4] The detonation synthesis is now an established technique for the production of <10 nm ND particles in commercial quantities.[5] Detonation NDs (DNDs) are ∼5 nm in diameter, nearly spherical diamond particles bearing many different functional groups on the surface due to the termination of sp^3 carbon dangling bonds in reactions with components of the environment.[6] Larger and smaller NDs are also present in DNDs in small fractions.[7] Larger DNDs can be isolated by selective burn out of smaller DND particles in controlled conditions in air,[8,9] a process similar to the air oxidation purification method of DNDs.[10] Other techniques have been developed for the synthesis of ND particles, albeit on a smaller scale: chemical vapor deposition,[11] laser ablation,[12,13] cavitation-assisted conversion,[14] and gas-phase plasma synthesis.[15] All of these techniques usually produce ND particles of ∼5 nm diameter or larger. Milling of micron-sized particles is also a commonly and commercially used technique for the fabrication of NDs but generally results in ≫10 nm-sized particles of highly irregular shapes and broad particle size distributions.[16] A recently reported fast and economical future alternative to milling is crushing of microdiamonds using the energy of an explosion.[17]

Received: January 19, 2022
Accepted: May 3, 2022
Published: May 23, 2022

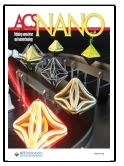

https://doi.org/10.1021/acsnano.2c00197
ACS Nano 2022, 16, 8513–8524

Small particle size is advantageous for many applications of NDs: in polymer matrix composites, a small size and spherical shape of nanofillers lead to a larger number of particles per unit of their mass and maximize the volume of the interphase in the composite;[18] in biomedical applications, the small size facilitates ND penetration through narrow pores in biological structures, such as nucleolemma and the kidney filtration system.[19] In general, the smaller the particle size, the higher the surface-to-volume ratio. This increase in surface area is accompanied by a change in chemical potential and overall reactivity and could be beneficial also for catalytic applications such as the direct reduction of CO_2.[20] Pushing the boundaries of these applications drives the practical interest in smaller ND particles of less than 5 nm. There is also a theoretical drive to produce sub-5 nm diameter NDs, as hydrocarbons with tetrahedral (diamond) structure were predicted[21] (and soon rebutted[22]) to be more stable than the corresponding hydrocarbons of hexagonal (graphene) structure at small sizes. This controversy, as well as a large uncertainty in the predicted size at which the stability crossover occurs (from ∼1.3 to ∼6.0 nm), invites further experimental investigations into the relative stability of diamond and graphene nanoparticles in this size range and with different surface terminations. A quantum confinement effect was also predicted for hydrogen-terminated NDs smaller than 2 nm.[23]

NDs can be fabricated or synthesized through either top-down or bottom-up approaches, as illustrated in Figure 1.

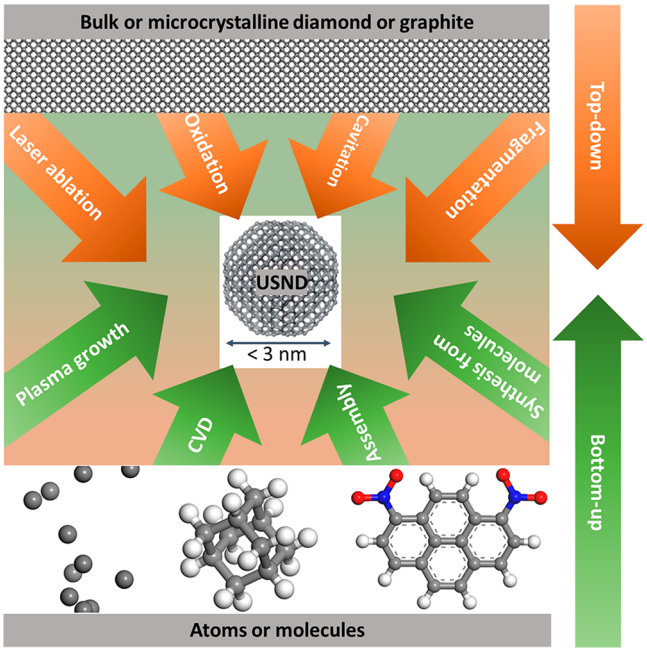

Figure 1. Schematic showing representative possible techniques for the synthesis of ultrasmall nanodiamonds (USNDs) using top-down and bottom-up approaches.

Several variations of air oxidation processes have been explored to reduce the size of NDs.[24] Controlled layer-by-layer removal of carbon atoms via oxidation in air reduced the size of DNDs from 5.2 to 4.8 nm.[25] More recent studies have reported ND size reduction to <2 nm by one-step controlled oxidation in air,[26] a variation of the process originally proposed for DND purification.[10] These techniques represent examples of the top-down approaches to ultrasmall NDs (USNDs), which we define for the purposes of this perspective as NDs with a size <3 nm in all dimensions.

On the opposite end, there are the bottom-up ND synthesis techniques (Figure 1), which may provide a better control over size, purity, and surface chemistry of the ND particles. Moreover, the development of a bottom-up chemical synthesis of NDs may help us understand diamond genesis on Earth[27] and in space. In addition, bottom-up synthesis of NDs from molecular precursors remains a long-standing challenge for synthetic organic chemists. It should be mentioned on this conjunction that the difference between bottom-up and top-down methods is not always clear. For example, laser ablation starts from a bulk carbon precursor, but in the process, carbon atoms or small clusters evaporate, and the resulting diamond structure is formed from these smaller fragments.

From the synthesis of adamantane by Prelog in 1941 to the wet chemical synthesis of higher homologues, chemists have struggled with obstacles such as poor solubility and selectivity and a large number of very similar isomers rendering the isolation of pure diamondoids a formidable challenge.[28] Filling the ∼4 nm gap in size between the largest presently synthesizable diamondoid and a typical DND particle (Figure 2) invites further efforts. An interesting recent study has reported a synthesis of sub-4 nm NDs from graphene oxide and nitrated polycyclic aromatic hydrocarbons at 423 K and ambient pressure.[29] Below, we discuss this and other approaches to synthesize USNDs, some of their properties and potential applications, as well as related advantages and challenges. Of particular interest for this perspective are the bottom-up synthesis methods of diamonds, NDs, and USNDs, while the readers interested in details of the top-down techniques are referred to the corresponding publications cited throughout this perspective. A table summarizing bottom-up synthesis techniques of NDs and USNDs is also available in the Supporting Information accompanying ref 29. Several of these techniques are still in their infancy. However, the broad choice of techniques and better control achieved with bottom-up methods hold promise for the synthesis of tailored diamond particles of bespoke size and morphology, perfectly adapted to the intended applications.

ULTRASMALL ND: MOLECULE OR NANOPARTICLE?

Humans have been unintentionally producing nanoparticles since time immemorial, at least since they started to burn wood.[30] In retrospect, many human-made materials used before the advent of the official era of nanomaterials should have also been properly called nanomaterials. DND was first produced in the 1960s and was known under the names “ultradispersed diamond”, “ultrafine dispersed diamond”, etc.[4] until the term “nano-” became broadly used in materials science, and all these names have changed to “nanodiamond”. However, the science of nanomaterials was launched by the discovery of not a material but a molecule, C_{60}.[31] The discovery of C_{60} brought the world of nanoparticles and molecules in direct contact, blurring the line separating them and leading to conceptual questions as to how we define a molecule or a macromolecule and how we define a nanoparticle. Molecules are often perceived as objects that are smaller than nanoparticles, but given that some molecules are >5 nm in size[32] while many nanoparticles are significantly smaller, size alone cannot be a defining property (Figure 2).

One may choose fixed composition as the criterion distinguishing molecules (the smallest units of a substance that retains its fixed chemical composition represented by a well-

https://doi.org/10.1021/acsnano.2c00197
ACS Nano 2022, 16, 8513−8524

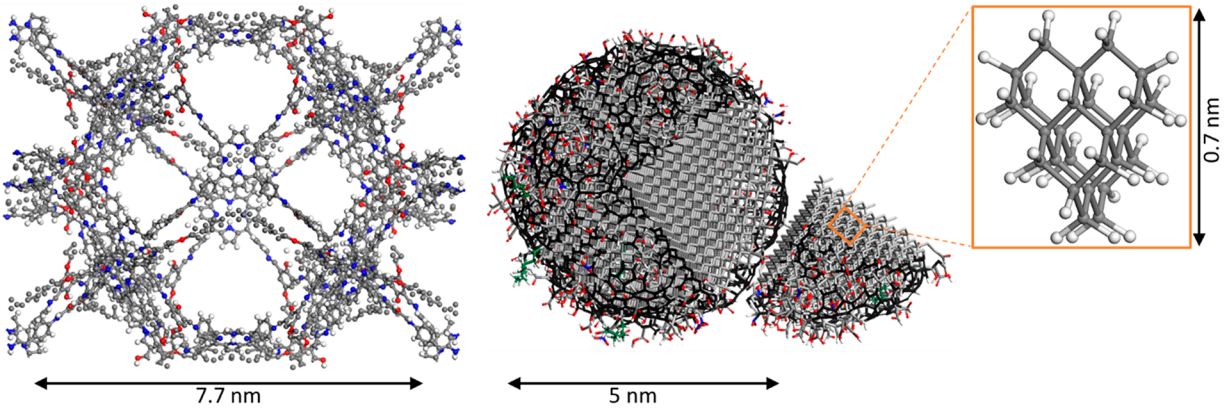

Figure 2. Optimized atomistic models illustrating structures and sizes of some molecules and nanoparticles: (left) one of the largest synthesized molecules, 7.7 nm diameter tetracosakis([2-hydroxy-5-(octyloxy)-1,3-phenylene]dimethylidene)dodecakis(5,10,15,20-tetrakis(4-aminophenyl)porphyrin), $C_{912}H_{841}N_{96}O_{48}$;[33] (middle) 5 nm diameter DND particle illustrating the diamond structure in the core and different types of functional groups and sp^2 C on the surface; and (right) [1(2,3)4]pentamantane, $C_{26}H_{32}$, a representative of diamondoids, which are hydrocarbon molecules that can be thought of (without hydrogens) as building blocks of a diamond crystal structure.

defined molecular formula) from nanoparticles (small particles without a fixed composition and without a well-defined molecular formula). However, the existence of macromolecules challenges this criterion, as well, as polymer macromolecules often lack a fixed chemical formula but have a fixed ratio of their constituent elements. Yet another more application-oriented approach is to define a molecule as the smallest unit of the substance that retains its characteristic properties. This approach is challenged by the question: what properties should we choose as characteristic properties of a substance? The question is especially important as many properties of nanoparticles significantly differ from the properties of larger particles and bulk materials: melting point[34] and thermodynamic properties,[35] optical properties,[36,37] catalytic properties,[38] and many other properties of materials depend on the size of their particles. To make things even more complicated, this dependence is more pronounced at very small sizes. Other characteristics can also be considered to distinguish molecules from nanoparticles, for example, whether electron energy levels in a small object form separate discrete energy levels, as in molecules, or continuous energy bands, as in crystals and other solids. This approach is challenged by similarities between the quantum mechanical methods of describing electronic structure of molecules and crystals.[39] The important conceptual question ("molecule or nanoparticle?") needs further discussions, and until a broader consensus is reached, in this perspective, we will stick with fixed composition criterion and call small particles of diamond, including those of sub-5 nm size, nanoparticles, not molecules, while all presently available diamondoids that can be assigned a definite chemical formula will be distinguished as molecules (Figure 2).

NONDETONATION SYNTHESIS AND GROWTH OF DIAMOND

Detonation synthesis of NDs is now an established commercial production technique and was reviewed before.[6] Other methods of ND synthesis are also being researched and developed. The direct synthesis of diamond from carbon atoms has fascinated researchers for a long time. Moissan dissolved carbon precursors in molten iron in his attempts to produce diamond.[40] Later, Leypunskiy concluded that it might be easier to form diamond from carbon atoms dissolved in molten metals where they are more mobile compared to carbon atoms in the crystal structure of graphite.[41] Potential carbide formation may also contribute to an increased "solubility" of carbon in molten metals. Most of the modern diamond synthesis methods use solutions of a carbon precursor in molten metals at high temperatures and pressures[42] (HPHT diamond) or even at ambient pressures and temperatures below 1000 °C (20 nm to 150 μm diamonds were produced by this technique[43]). In addition, it is often hypothesized that some metals act as catalysts of diamond formation, not merely as solvents. As-synthesized HPHT diamond particles are generally well above 10 μm in size. Size reduction of commercial HPHT particles to less than 10 nm is possible,[44,45] but the fabrication processes known today are generally very inefficient and not scalable.

Many attempts to synthesize diamond were focused on extreme pressure (P) and temperature (T) conditions, being guided by the graphite−diamond equilibrium line on the phase diagram of carbon, which shows that, at any given T, diamond is more thermodynamically stable than graphite when P is higher. However, the transition from graphite to diamond is not a simple polymorphic transition (i.e., it is not just a change of crystal structure) but a chemical reaction,[46] consisting of breaking the aromatic covalent bonds in graphite and forming new single covalent bonds in diamond, accompanied by the corresponding changes in hybridization (electronic state) of C from sp^2 to sp^3. Breaking strong covalent bonds requires significant energy, usually provided in the form of heat, and therefore, very high T values are needed for direct graphite to diamond transition. In line with this thinking, HPHT and other techniques capable of reaching high P and T were explored for ND synthesis. One example is cavitation, which produced 10−30 nm NDs identified via electron diffraction patterns and Raman spectra.[47] High P induced by cavitation in a Venturi tube was mentioned as the main reason for diamond formation. Later, ultrasound cavitation was used to produce 5−10 μm diamond particles from graphite suspended in liquid aromatic oligomers $C_nH_mO_x$ (n = 18−36; m = 14−26; x = 2−5).[14] The authors also cite high P and T conditions in cavitation bubbles formed by a powerful ultrasound source as necessary for diamond phase formation.

While the direct transition from graphite to diamond requires high P and T, it does not mean that diamond synthesis from other precursors necessarily requires high P and T, especially in

https://doi.org/10.1021/acsnano.2c00197
ACS Nano 2022, 16, 8513−8524

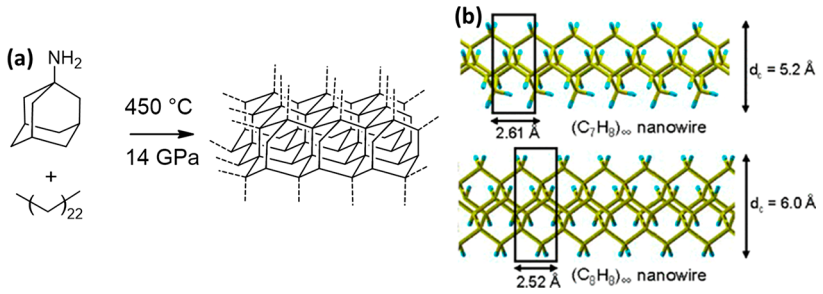

Figure 3. Examples of proposed synthetic pathways from molecular precursors to diamond and diamond-like materials: (a) mild HTHP conditions for the growth of nanodiamond from aminoadamantane seeds[58] were proposed to proceed via decomposition of tetracosane and intermediate formation of diamantane; (b) structures proposed for diamond nanowires formed from adamantane monomers encapsulated inside a double-walled carbon nanotube at temperatures of about 550 °C in vacuum. Reprinted from ref 57. Copyright 2012 American Chemical Society.

case of ND and USND, where the growth of large crystals is not the goal. The thermodynamics of a chemical reaction depends on the difference between the thermodynamic functions of products and reagents and is not directly related to the thermodynamics of solid-state graphite−diamond transition. The kinetics of a chemical reaction depends on the energy of the transition state of the reaction, which may be very different from transition states involved in the direct graphite−diamond transition. In other words, in principle, synthesis of diamond and ND should be possible in various P and T conditions, including very different from those on the graphite−diamond equilibrium line in the phase diagram of carbon. Thus, in principle, the right choice of precursors and chemical reactions may thermodynamically and kinetically favor diamond formation at given P and T, enabling diamond synthesis in milder conditions, sometimes in the presence of a proper catalyst, as noted previously.[46,48] Not surprisingly, there are many examples of ND synthesis from various carbon-containing precursors in conditions milder than the P and T of a direct graphite−diamond transition.

One interesting example is a recent publication,[29] where the authors emphasize the importance of the right choice of precursor (a nitrated polyaromatic compound in this case) based on mainly "chemical" considerations; i.e., the functional group induced partial rehybridization of sp^2 to sp^3 carbon has lowered the bond strength in the precursor structure, in this way facilitating the conversion of a polyaromatic compound to USND. Many different chemical vapor deposition (CVD) diamond film synthesis techniques are another example. Naturally, adamantane and diamondoids should be suitable nucleation seeds for diamond growth by CVD, based on structural similarities (Figure 2). The terminal C atoms in these molecules are bonded to H, as is also common for the growing crystallites of diamond in a CVD reactor using a hydrogen/methane mixture. Indeed, by optimizing the distance from the plasma source in a vertical microwave plasma-enhanced CVD reactor, it was possible to grow high-quality ∼10 nm single NDs with incorporated dopants starting from pentamantane seeds anchored to a substrate.[49] Adamantane, the smallest diamondoid, was also used as a seed for diamond growth on substrates,[50] where it not only acted as a nucleation site but also decomposed under the CVD conditions, forming other species of carbon, which could then in their own right act as seeds. However, the resulting NDs were less perfect compared to the former work. In principle, any diamondoids and their combinations can be used as seeds for epitaxial diamond growth. Their different shapes may provide a means to control the morphology of the growing diamond crystallites.[51]

Other precursors and techniques beyond CVD were also used to make ND particles. Gogotsi et al. observed 2−10 nm NDs embedded in amorphous/graphitic carbon after 24 h treatment of α-SiC in Ar/Cl_2 gas mix at 1000 °C. Addition of H_2 to the mix promoted formation of sp^3 C and produced hard diamond-structured film on SiC crystals.[52] This work sparked interest in ND synthesis by chlorination of carbides, with one of the most recent publications reporting synthesis of NDs (<10 to <50 nm) of different types by chlorination of TiC doped with catalytic amounts of Ni, Co, and Fe at 1000 °C.[53] Synthesis of NDs in the gas phase has also been reported. Sankaran et al. synthesized 2−5 nm NDs with cubic, n-diamond, and lonsdaleite crystal structures by dissociation of ethanol vapor in a low temperature (<100 °C) microplasma. Addition of H_2 to the ethanol vapor further improved product purity, producing NDs of similar particle sizes and crystal structures with less amorphous carbon.[15] The authors of this paper also noted that the diamond Raman peak of their USNDs (∼2.5 nm diameter) must be significantly down-shifted and broadened compared to that in the bulk diamond according to the predictions of phonon confinement model.[9] Similar changes in Raman spectra with ND size have been observed in other studies, as well,[54] and are discussed and illustrated in figures in the characterization section below. Other techniques have been proposed for ND synthesis in the gas phase, albeit at higher T. NDs and microdiamonds were collected on Cu-coated Si wafers exposed to an acetylene−oxygen torch flame. The NDs were identified by SEM and Raman spectroscopy by sharp peaks at 1334−1342 cm^{-1} assigned as diamond peaks up-shifted due to stress caused by the mismatch of the diamond crystal lattice and the structure of the substrate. However, no information about the size of the NDs produced by this method was provided, and their presence in the samples was not reliably confirmed.[55] In yet another variation of torch synthesis, transmission electron microscopy (TEM) analysis of the particles filtered from a common candle flame through a nanoporous alumina membrane detected 2−5 nm NDs surrounded by layers of graphitic carbon and embedded into amorphous carbon matrix.[56]

Another exciting opportunity to produce NDs would be the direct assembly of diamondoid molecules into larger diamond structures (Figure 3a,b). While this approach has yet to be realized, the feasibility of direct assembly of larger structures from diamondoids has been demonstrated by coalescence of adamantane confined inside a carbon nanotube upon heat treatment (Figure 3b).[57] However, in this case, linear carbon

https://doi.org/10.1021/acsnano.2c00197
ACS Nano 2022, 16, 8513−8524

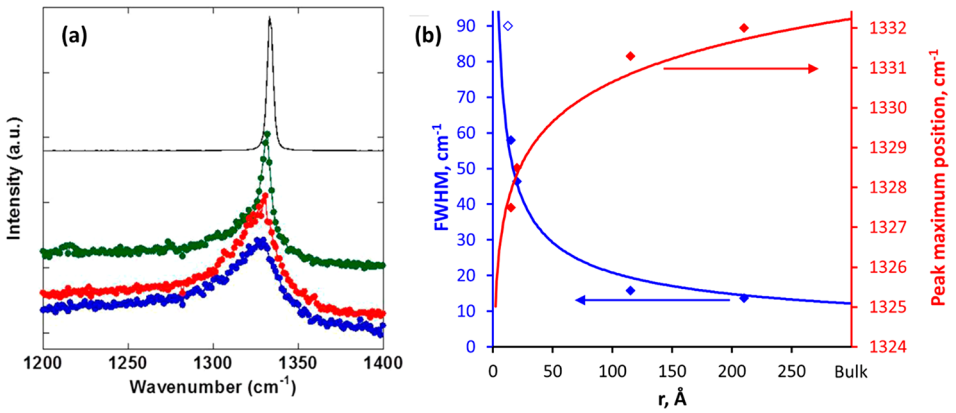

Figure 4. Raman spectroscopy of NDs: (a) first-order "diamond line" of three commercial DNDs (blue, NanoCarbon Research Institute, Ltd., mean size 3−5 nm; red, PlasmaChem, grain size 3−6 nm; green, Sinta, mean size 4−8 nm) and the reference diamond single crystal (black) (reprinted with permission from ref 64; copyright 2018 Elsevier); (b) position and full width at half-maximum (fwhm) of the "diamond line" for NDs of different radii and bulk diamond (filled[66] and open[15] symbols are experimental data, lines are guides for the eye only).

chains were formed, and the diamond-like properties were lost. This could indicate that 1D structures with the width of one adamantane molecule, in general, do not possess the properties of diamond.

As mentioned above, the bottom-up synthesis of diamond from organic precursors can lead to a much more precise control over composition and structure of the resulting particles. Along these lines, one option is to replace the graphitic precursor in HPHT synthesis with organic molecules. Kawamura and Ohfuji used stearic acid for the HPHT synthesis of 10 nm diamonds in mild conditions (1000 °C, 13−17 GPa).[59] However, the proposed mechanism stipulates the intermediate formation of highly disordered graphitic material, and therefore, this method is not an actual bottom-up synthesis from the organic precursor. This might also be true for other reported "wet chemical" syntheses from molecular precursors. The high energies involved in these techniques exceed the thermal stability window of the precursors, inducing their transformations prior to the actual formation of diamond. One example of such a process that was reported to yield small diamond-like particles is a very violent reaction of tetrachloromethane with alkaline metals in the presence of a Ni−Co catalyst[60] (Attention! This experiment is the source of many extremely dangerous laboratory accidents, when chlorinated solvents are accidentally dried with alkaline metals!) Another small molecule precursor for diamond synthesis is carbon dioxide.[61] In this case, micron-sized diamond particles were also obtained in a reductive procedure involving metallic sodium. In a more indirect manner, CO_2 initially transformed into Li_2CO_3 was encapsulated in a carbon layer and then thermally transformed into ND crystallites covered by multilayer graphitic shells.[62] These structures resemble bucky-NDs[63] obtained by careful thermal annealing of nanoscale diamond, although the interface between the diamond and the nondiamond shell is entirely different as it existed prior to the formation of the diamond core.

CHARACTERIZATION OF NDs AND ULTRASMALL NDs

As the size of NDs becomes smaller, their reliable characterization becomes more challenging because (i) their properties deviate more from the known properties and characteristic features of bulk diamond and even from more familiar larger NDs, making correct assignment of the analytical signals problematic, and (ii) the USNDs produced by certain techniques (such as chlorination of carbides[52] or low-T conversion of nitrated graphene[29]) are inevitably embedded in a difficult to remove matrix of nondiamond carbon and other byproducts, which in combination with the very small size of these NDs (i.e., low intensity of the analytical signal) poses additional challenges to their characterization. For larger NDs (>10 nm diameter), well-established techniques are available for the characterization of crystal and electronic structures and vibrational signatures. These include X-ray or electron diffraction, Raman spectroscopy, and TEM. Powder X-ray diffraction gives peaks at positions corresponding to the crystal plane spacings. The width of the peaks can be correlated to the size of coherent scattering domains via the Scherrer equation or Williamson-Hall analysis.[8,17] However, characterization and even detection of USNDs (≪5 nm) by diffraction becomes ambiguous due to a smaller size of the scattering domains as well as larger deviations of their structure from the known structure of bulk diamond combined with larger variations in the interatomic distances in a small nanoparticle compared to a bigger crystal. Further problems arise if NDs are embedded in a disordered or amorphous carbon matrix as the analytical signal from the matrix may be significantly higher than the signal from embedded particles.

Raman spectroscopy is one of the most popular techniques for distinguishing carbon allotropes. Diamond is typically identified via the so-called "diamond line" at ∼1332 cm^{-1}, the first-order Raman-allowed degenerate T_{2g} mode of diamond. At the nanoscale, particle size and strain can lead to sample-specific changes in the position and shape of this peak compared to bulk diamond[54,64] (Figure 4a). The diamond line in NDs demonstrates asymmetric broadening and shifting toward lower wavenumbers, both effects becoming much more pronounced for USNDs (Figure 4b) due to superposition of the optical phonons of crystalline diamond around the Γ-point,[9,65,66] as explained within the phonon confinement model. On the other hand, for USNDs, a simple phonon confinement interpretation of the diamond line can be inadequate, in part due to a high strain as well as a larger contribution of surface terminations to the spectral signature of USNDs.[67] Unlike these "bulk" characterization techniques, TEM is capable of probing the geometric and electronic structures of materials "locally" at the atomic scale. It provides structural information based on diffraction and high-resolution imaging, as well as chemical and bonding information via electron energy loss spectroscopy

https://doi.org/10.1021/acsnano.2c00197
ACS Nano 2022, 16, 8513−8524

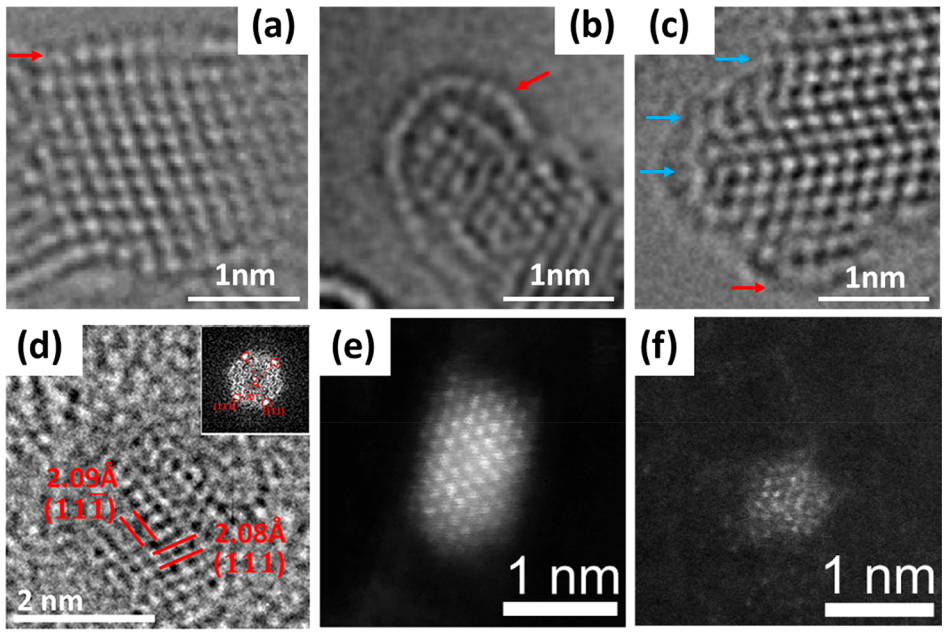

Figure 5. Imaging of NDs: (a−c) HRTEM images of DNDs of varying sizes, showing the diamond structured core and reconstructed surfaces (red arrows). Blue arrows indicate the twin planes within the particle (reprinted with permission from ref 69; copyright 2018 Royal Society of Chemistry); (d) HRTEM image and its corresponding amplitude of Fourier transform (inset) of a ∼2 nm USND synthesized in mild conditions from nitrated naphthalene. The USNDs are embedded in amorphous carbon and residual precursors (reprinted from ref 29; copyright 2021 American Chemical Society); (e,f) annular dark-field scanning transmission electron microscopy image of 1−2 nm NDs showing *only* the core of the particles (reprinted with permission under a Creative Commons CC BY License from ref 26; copyright 2016 Springer Nature.

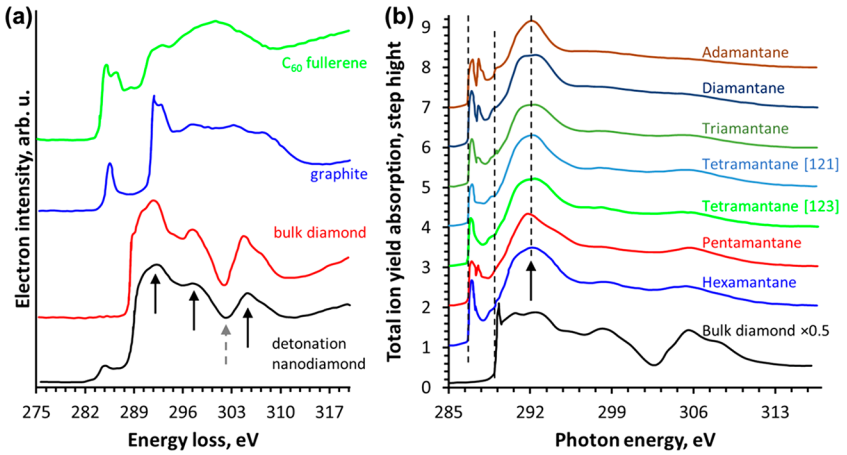

Figure 6. Electronic structure of NDs: (a) EELS carbon K-edge of carbon materials: DND (black), single crystal diamond (red), graphite (blue), and C_{60} (green). The black arrows in diamond EELS spectra indicate the three characteristic peaks for transitions from 1s bound states to the unoccupied p states in diamond, and the dashed arrow indicates the "second gap" in the diamond band structure (adapted with permission under a Creative Commons Attribution 3.0 Unported License from ref 72; copyright 2016 Royal Society of Chemistry); (b) XAS of carbon K edge of diamondoids from adamantane to hexamantane (adapted with permission from ref 76; copyright 2005 American Physical Society).

(EELS). The major advantage is that such information comes from a specifically targeted volume of the sample, in favorable cases down to a single atom level. This is important for particles embedded in a matrix as one can selectively record the signal from a nanoparticle.[29,68] Hence, TEM is an indispensable characterization tool for USNDs.

Figure 5a−c shows high-resolution TEM (HRTEM) images of single DNDs ranging from 1.8 to 4 nm in size and exhibiting well-resolved atomic columns of the diamond core and a single layer of atoms constituting reconstructed surfaces resembling fullerene-like structures.[69] Surface reconstruction has been predicted for USNDs by density functional calculations.[23,70] Experiments with NDs of different origins (e.g., from meteorites[71]) support these observations. The core−shell structure of ∼5 nm NDs can be further corroborated by the EELS carbon K-edge spectra[72] or X-ray absorption spectroscopy (XAS)[23] (Figure 6). The diamond core gives characteristic EELS peaks for electron transitions from 1s bound states to unoccupied p states in diamond (Figure 6a, solid black arrows) at 292 (the σ^* peak), 297, and 305 eV and a dip at ∼302 eV corresponding to the "second gap" in the diamond band structure. The fullerene-like reconstructed surface is represented by the near-edge structure energy losses at 284−288 eV, where the pronounced peak at ∼284.5 eV corresponds to the transitions to the π^* state.[23,72] The additional minor peaks at 285−288 eV can have multiple origins: surface chemical bonds

https://doi.org/10.1021/acsnano.2c00197
ACS Nano 2022, 16, 8513−8524

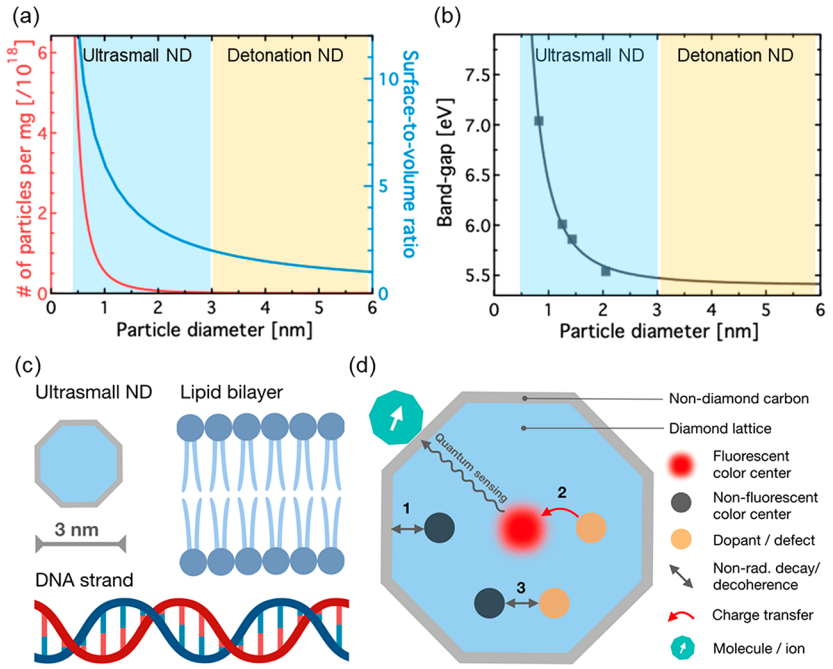

Figure 7. Technological advantages of tailored USNDs: (a) calculated number of particles per milligram and surface-to-volume ratio for spherical diamond particles as a function of particle diameter, showing that both characteristics rapidly increase in the USND size range; (b) predicted band gap of nanodiamonds as a function of particle diameter;[91] (c) schematic illustration of a 3 nm ND and parts of a lipid bilayer and DNA double strand drawn to scale; (d) schematic illustration of color centers in a ND and their interactions with different parts of the particle and its environment (see text for explanation).

(C−O, C−H),[73,74] defects (pentagonal rings linking the shell to the diamond core and accommodating surface curvature),[23] etc. It is important to emphasize that the information about the atomic structure obtained from the TEM image and the information about electronic structure obtained from EELS must be consistent to ensure an accurate confirmation and interpretation of both the surface and diamond core of the ND structure.[69,71,72] For USNDs smaller than 1−2 nm, important fundamental questions arise regarding their electronic structure, which also have implications for their characterization. Given that theoretical calculations predict a significant increase of the band gap with decreasing size[23,70,75] (Figure 7b), should we expect the electronic structure of such USNDs to closely resemble bulk diamond? In the ultrasmall size range, the fraction of surface atoms becomes greater than the core (Figure 7a), and the surface states likely begin to dominate.

In this limit, the electronic structure of NDs may become more similar to that of diamondoid molecules, which has been analyzed and compared to bulk diamond using XAS (Figure 6b).[76] The differences between diamondoids and diamond are clear in XAS. First there are multiple peaks in the near-edge region (285−289 eV), reflecting the dominating "surface states" due to CH and CH_2 groups.[77] The peaks associated with transitions to σ^* are shifted, whereas the two other characteristic peaks and the "second gap" dip (indicated by the solid black and dotted gray arrows in Figure 6a) are either very weak (for higher diamondoids pentamantane and hexamantane) or absent. The σ^* feature of diamondoids resembles that of hydrocarbon molecules.[78] Thus, electronic structure measurements provide another powerful and perhaps crucial tool to observe distinct diamond signatures. In cases where USNDs are embedded into a matrix, the sensitivity of HRTEM and annular dark-field scanning transmission electron microscopy (ADF-STEM) imaging to crystalline structure becomes very useful. This sensitivity achieved via real-space selectivity (i.e., direct probing/visualizing area of interest to better than 0.1 nm resolution) is generally superior to X-ray or electron diffraction.

For example, ∼2 nm NDs formed in mild conditions from nitrated polycyclic aromatic hydrocarbons[29] and embedded in an amorphous carbon matrix were revealed by HRTEM (Figure 5d), demonstrating the selectivity and sensitivity of TEM imaging (although the electronic structure from EELS does not show the characteristic diamond C−K edge fine-structure signatures). In another study, ADF-STEM (Figure 5e,f) clearly resolved the cores of 1−2 nm NDs.[26] However, as ADF-STEM imaging contrast is dominated by the crystalline structure, the details of surfaces may not be visible. Moreover, EELS for the embedded/supported particles is very challenging as the particle signal can be overwhelmed by the signal from the matrix/support, particularly if the latter are also carbon materials, as is often the case for USNDs. While it is possible to only collect the signals from the ND "region", the projection criteria (the volume of material over which the electron beam transmit is integrated and projected into 2D) mean that the signal from the matrix/support on top or bottom of the "region" is tangled with the ND signal.

Additional challenges are presented by the sources of excitation of the chosen characterization method. High local excitation laser intensities in Raman spectroscopy are known to damage NDs, necessitating the use of low laser powers (total beam power in the μW range) and long acquisition times. The ability of TEM to probe very small volumes of materials also brings about limitations. The medium voltage (100−300 kV) electron beam irradiation can damage the ND surface, whereas prolonged irradiation can transform diamond into graphite.[79] Therefore, lower electron beam energy (60−80 kV) reducing the knock-on damage is preferred for TEM work with NDs.[69,72] However, even with low beam energies, the high incident

https://doi.org/10.1021/acsnano.2c00197
ACS Nano 2022, 16, 8513−8524

fluences (>1000 e^-/A^2) often required for HRTEM and EELS can still change the intrinsic structure of the NDs and especially USNDs. Recent advent of direct electron detection cameras in TEM enables imaging and EELS at ~100 times lower electron beam dose, allowing direct imaging of radiation-sensitive materials in TEM. These emerging capabilities will undoubtedly prove very useful for overcoming some of the difficulties in characterization of the USNDs.

ADVANTAGES OF BOTTOM-UP SYNTHESIS OF ULTRASMALL NDs FOR APPLICATIONS

Besides the theoretical and synthetic importance of the USNDs, they offer great potential for many applications—another important reason for making and studying them. Extremely large surface-to-volume ratio, ultrasmall size, and nearly spherical shape are critical for many applications from nanocomposites[18] to drug delivery.[19] In the context of nanocomposites, a smaller particle size translates into a larger number of ND particles per 1 g of material, i.e., a lower mass concentration of the nanoparticles in the matrix required to achieve same improvements in properties of the nanocomposite as compared to the particles of a larger size. When the particle diameter drops below 5 nm, the surface-to-volume ratio and the number of particles per unit mass grow very rapidly with decreasing particle diameter (Figure 7a). Particle size is critical for biological applications as it determines some of the particle's intrinsic properties such as its diffusion coefficient and strongly influences many interactions with biological systems (e.g., biodistribution and clearance) and with biomolecules. For example, USNDs are smaller than the thickness of the lipid bilayer that forms the membranes of most biological cells and are comparable to the diameter of a DNA double strand (Figure 7b). USNDs may be able to access biological compartments that most other nanoparticles cannot and cross barriers such as the nucleolemma and the blood−brain barrier, possibilities rendering them material of choice for emerging drug delivery[80] and theranostic applications.[19,81] While larger 30 nm fluorescent NDs have been demonstrated to be useful to track intracellular transport in neurons,[82] they are not suitable to track objects that are significantly smaller (e.g., many proteins) than the fluorescent ND beacon. USNDs would greatly expand the range of biological objects that can be fluorescently labeled and tracked with NDs. Many biological and sensing applications require fluorescent NDs. In this context, the bottom-up synthesis of USNDs may provide opportunities to create and tailor the properties of fluorescent NDs in the future. Fluorescence from atomic defects or "color centers" like the nitrogen vacancy (NV) center is the basis for a vast array of emerging imaging and quantum sensing approaches. Yet today, fluorescent defects in <10 nm NDs cannot be created controllably or efficiently. While small 3−5 nm sized DNDs are already useful for many other applications, they contain mostly nonfluorescent lattice defects whose location and composition cannot be controlled.[83] Many types of DNDs do show fluorescence, but it generally originates from surface-related defects and is neither photostable nor useful for quantum sensing.[83] A wet chemical bottom-up synthesis of NDs from molecular precursors can lead to NDs with precisely defined defect composition, concentration, and location in the structure of the particle. This may result in a hitherto unknown class of nanoscale light sources and quantum sensors, leading to a paradigm shift in the field of ND science and technology. While hundreds of fluorescent defects in diamond are known,[84] only a few (e.g., the NV and other N-related defects,[85] SiV and GeV,[86] substitutional Ni[87]) can be reliably fabricated in NDs. In commercial 10 nm NDs, NV centers can be created with a yield of <10% at best (i.e., only one in 10 NDs contains an NV center).[88] Several other defects can be fabricated in small quantities in larger (≫10 nm) top-down synthesized NDs for proof-of-concept experiments, but not for applications. Particles with sub-10 nm size that host stable color centers have been reported,[45,89,90] but reliable and scalable fabrication methods do not yet exist.

Some key mechanisms that currently restrict our ability to efficiently create USNDs with fluorescent color centers are illustrated in Figure 7d: (1) Interactions of color centers with surface states can quench fluorescence completely, e.g., via energy or charge transfer, and reduce spin coherence times. (2) Charge transfer between color centers and other dopants is often required to create the desired so-called "charge state" of the color center (in case of the NV center a nearby substitutional, N often donates an additional electron to create the desired NV^-, whereas in the absence of an electron donor, the NV center cannot be used for sensing). (3) Interactions between color centers and other dopants can lead to spin decoherence or fluorescence quenching (excess of N in the vicinity of NV centers causes magnetic noise that reduces the coherence time of the NV^- electron spin[92] and the sensitivity of quantum sensing and can also lead to fluorescence quenching[93]). As a result, state-of-the-art ND quantum sensing experiments such as magnetometry and thermometry based on optically detected magnetic resonance (ODMR) of NV centers generally employ particles with a diameter well above 50 nm.[94] However, ODMR for NDs below 10 nm in size has been demonstrated,[95] and simulations suggest that fluorescent NV centers can exist in NDs with less than 1.5 nm diameter.[96,97] For the negatively charged silicon vacancy center (SiV^-), fluorescence from 1.6 nm-sized particles has already been demonstrated,[89] highlighting the potential of color centers other than the NV center in USNDs. All this suggests that many current limitations in ND-based quantum sensing are mainly due to our lack of control over the exact composition of particles.

In the next generation of small and sensitive diamond-based quantum sensors, all of the interactions illustrated in Figure 7d as well as the color center location in the particle must be controlled. A bottom-up chemical synthesis (Figure 1) may enable this, while currently available techniques allow almost no control at the single particle level. Therefore, our ability to precisely control the concentration and location of color centers in USNDs through the properties and combination of precursor molecules becomes critical. It would potentially allow for the precise incorporation of well-known defects like the NV center, the incorporation of known defects that have so far been challenging to fabricate, and the exploration of other, completely unknown color centers. Another exciting opportunity provided by a precise bottom-up synthesis of NDs is the combination of many color centers in one USND particle (≪5 nm). In the context of bioimaging, these particles would potentially combine some of the outstanding properties of molecules with the unique properties of a diamond-based solid-state system: they would be able to access almost all locations within biological systems like molecules and at the same time enable all optical quantum sensing experiments due to the extreme photostability of fluorescent defects in diamond. Precise synthesis would allow the introduction of many fluorescent color centers in each ND and ensure their sufficient brightness for fluorescence imaging.

https://doi.org/10.1021/acsnano.2c00197
ACS Nano 2022, 16, 8513−8524

Full control over the particle defect composition could enable the creation of color centers with long spin coherence times and stable charge states even in USNDs. Due to the ultrasmall particle size, these color centers will strongly couple to the particle environment (Figure 7c,d), enabling precise quantum sensing. On the opposite end of the spectrum of possibilities is the option of making USNDs containing only a single color center per particle. Such USNDs could enable quantum imaging based on single photon emission.[98] Assembly of these particles in photonic structures could enable the design of scalable quantum computing circuits that do not require the fabrication of individual single photon emitters using costly and time-consuming top-down techniques. In principle, the spin of individual electrons inside USNDs could be used for all-optical nanoscale quantum sensing based on defects with spin-dependent fluorescence like the NV center.

CONCLUSIONS AND OUTLOOK

A brief and by far incomplete overview of selected efforts and recent activities in the area of synthesis of nanodiamond particles, especially of ultrasmall NDs provided above, shows that this is an important and timely topic of research. From the standpoint of physics and materials science, this research may clarify some fundamental and still debated aspects of the relative stability of sp^2 versus sp^3 carbon structures at the nanoscale. The wet chemical synthesis of diamond structure from molecular precursors in mild conditions will also provide a long-awaited methodological breakthrough in synthetic chemistry. Filling up the "USND gap" between diamondoid molecules and larger NDs will ultimately contribute to our understanding of fundamental differences (or lack of thereof) between molecules and nanoparticles, potentially bearing implications for fundamental research far beyond the area of diamond and carbon structures. Practical advantages of USNDs are also obvious. Synthesis of USNDs in mild conditions from well-defined molecular precursors will provide the means for precise tuning of the properties of interest of these particles, ranging from their size and surface chemistry, which define their behavior and fate in biological environments, to their electronic, spin, and luminescent properties, which are now attracting increased interest for quantum sensing, imaging, biomedical, and other applications. Stability and degree of interaction with the environment of the known and yet to be discovered color centers in USNDs can be tuned by a proper choice of molecular precursors and parameters of their assembly process to precisely tailor the distance of these centers from the particle surface and from each other. For example, one may envision simultaneous covalent bonding (cross-linking) of preassembled molecular structural units bearing desired functional groups in well-defined positions (e.g., reactive diamondoid derivatives, Figure 1), leading to instantaneous formation of a diamond structure in a process somewhat similar to epoxy cross-linking. Although this wet chemical synthesis of USNDs from preassembled molecular precursors still remains to be demonstrated, recent reports have shown that it is possible to produce USNDs from nitrated polyaromatic molecules[29] and adamantane derivatives.[58,99] Further theoretical and experimental efforts are needed to fully understand the role of electron-withdrawing (nitro-) groups of the polyaromatic precursors in their conversion to diamond.[29] The effects of the environment (or catalysis) on this conversion also need a better understanding. In general, a variety of "chemical" aspects of diamond synthesis discussed above need more attention in the future. Another interesting direction of future research on diamond synthesis may be related to diamond formation in 2D transition metal carbides (MXenes), following the research on diamond formation in bulk carbides and merging it with the novel and quickly developing area of MXene research. The potential benefits of this combination are as follows: (a) reducing the diamond synthesis from bulk carbides to the nanoscale forms of carbides will result in a better control over their size (the produced USNDs cannot be bigger than the thickness of the precursor MXene flake, which can be controlled at the nanoscale with virtually atomic precision); (b) the purity of the USNDs produced from MXenes should be higher, facilitating USND isolation and purification (due to the nanoscale form of the precursor the mass of unreacted carbide and byproducts is expected to be lower compared to a bulk carbide precursor); (c) the synthesis of USNDs from carbonitride MXenes may provide an unexplored way to USNDs with NV centers with potentially better control over their concentration and distribution in the resulting diamond structure, which will be determined by the structure and composition of the carbonitride MXene. Another direction of the future USND research should be related to finding better ways for their isolation from the matrix and reliable characterization. In terms of characterization, our progress will be obviously linked to technological advances in transmission electron microscopy and atomic scale spectroscopy. As discussed above, the next generation of instrumentation and detectors will provide more opportunities in this regard. In parallel, theoretical and experimental studies (with more accurate and sophisticated interpretation from theoretical calculations) of vibrational, electronic, optical, luminescent, and other properties of NDs depending on their size, especially in the size range below 5 nm, where these properties quickly change, should be continued. These studies will not only provide better understanding of fundamental physics of diamond in this size range but also guide our efforts in understanding and selecting the corresponding analytical signals to develop proper, more sensitive, less damaging, and more reliable ways of characterization.

Overall, recent progress in USND research has been encouraging, and the future of this field seems to be bright and important for fundamental science, as well as for the development of applications for ultrasmall diamond particles.

AUTHOR INFORMATION

Corresponding Authors

Vadym N. Mochalin − *Department of Chemistry, Missouri University of Science and Technology, Rolla, Missouri 65409, United States; Department of Materials Science and Engineering, Missouri University of Science and Technology, Rolla, Missouri 65409, United States;* orcid.org/0000-0001-7403-1043; Email: mochalinv@mst.edu

Shery L. Y. Chang − *Electron Microscope Unit, Mark Wainwright Analytical Centre and School of Materials Science and Engineering, University of New South Wales, Sydney, NSW 2052, Australia;* orcid.org/0000-0001-7514-4584; Email: shery.chang@unsw.edu.au

Philipp Reineck − *ARC Centre of Excellence for Nanoscale BioPhotonics & School of Science, RMIT University, Melbourne, VIC 3001, Australia;* orcid.org/0000-0003-1549-937X; Email: philipp.reineck@rmit.edu.au

Anke Krueger − *Institute of Organic Chemistry, University of Stuttgart, 70569 Stuttgart, Germany;* orcid.org/0000-0003-3082-4935; Email: anke.krueger@oc.uni-stuttgart.de

https://doi.org/10.1021/acsnano.2c00197
ACS Nano 2022, 16, 8513−8524

Complete contact information is available at:
https://pubs.acs.org/10.1021/acsnano.2c00197

Notes

The authors declare no competing financial interest.

ACKNOWLEDGMENTS

V.N.M. acknowledges partial support from the Synthesis and Processing of Materials program in the Army Research Office (Project W911NF-18-1-0155) and the National Eye Institute of the National Institutes of Health under Award Number 1R15EY029813-01A1. P.R. acknowledges support through an Australian Research Council DECRA Fellowship (Grant No. DE200100279) and a RMIT University Vice-Chancellor's Research Fellowship. S.L.Y.C. acknowledges support by the Australian Research Council (ARC) under Grant No. IC210100056. A.K. acknowledges the support by Deutsche Forschungsgemeinschaft (KR3316/6-2) and the BMBF (Project CarbonCat, Az. 033RC009B).

REFERENCES

(1) Vert, M.; Doi, Y.; Hellwich, K.-H.; Hess, M.; Hodge, P.; Kubisa, P.; Rinaudo, M.; Schué, F. Terminology for Biorelated Polymers and Applications (IUPAC Recommendations 2012). *Pure Appl. Chem.* **2012**, *84* (2), 377−410.

(2) *Nanotechnologies — Vocabulary — Part 2: Nano-objects*; ISO/TS 80004-2:2015(en), 2015; https://www.iso.org/standard/54440.html (accessed 2022-05-04).

(3) *Standard Terminology Relating to Nanotechnology*; ASTM E2456 - 06(2020); West Conshohocken, PA, 2020; DOI: 10.1520/E2456-06R20.

(4) Danilenko, V. V. On the History of the Discovery of Nanodiamond Synthesis. *Phys. Solid State* **2004**, *46* (4), 595−599.

(5) Dolmatov, V. Y.; Ozerin, A. N.; Kulakova, I. I.; Bochechka, O. O.; Lapchuk, N. M.; Myllymäki, V.; Vehanen, A. Detonation Nanodiamonds: New Aspects in the Theory and Practice of Synthesis, Properties and Applications. *Russ. Chem. Rev.* **2020**, *89* (12), 1428−1462.

(6) Mochalin, V. N.; Shenderova, O.; Ho, D.; Gogotsi, Y. The Properties and Applications of Nanodiamonds. *Nat. Nanotechnol.* **2012**, *7* (1), 11−23.

(7) Stehlik, S.; Henych, J.; Stenclova, P.; Kral, R.; Zemenova, P.; Pangrac, J.; Vanek, O.; Kromka, A.; Rezek, B. Size and Nitrogen Inhomogeneity in Detonation and Laser Synthesized Primary Nanodiamond Particles Revealed via Salt-Assisted Deaggregation. *Carbon* **2021**, *171*, 230−239.

(8) Osswald, S.; Havel, M.; Mochalin, V.; Yushin, G.; Gogotsi, Y. Increase of Nanodiamond Crystal Size by Selective Oxidation. *Diamond Relat. Mater.* **2008**, *17* (7), 1122−1126.

(9) Osswald, S.; Mochalin, V. N.; Havel, M.; Yushin, G.; Gogotsi, Y. Phonon Confinement Effects in the Raman Spectrum of Nanodiamond. *Phys. Rev. B* **2009**, *80* (7), 075419.

(10) Osswald, S.; Yushin, G.; Mochalin, V.; Kucheyev, S. O.; Gogotsi, Y. Control of sp^2/sp^3 Carbon Ratio and Surface Chemistry of Nanodiamond Powders by Selective Oxidation in Air. *J. Am. Chem. Soc.* **2006**, *128* (35), 11635−11642.

(11) Park, J.-W.; Kim, K.-S.; Hwang, N.-M. Gas Phase Generation of Diamond Nanoparticles in the Hot Filament Chemical Vapor Deposition Reactor. *Carbon* **2016**, *106*, 289−294.

(12) Pearce, S. R. J.; Henley, S. J.; Claeyssens, F.; May, P. W.; Hallam, K. R.; Smith, J. A.; Rosser, K. N. Production of Nanocrystalline Diamond by Laser Ablation at the Solid/Liquid Interface. *Diamond Relat. Mater.* **2004**, *13* (4), 661−665.

(13) Zousman, B.; Levinson, O. Pure Nanodiamonds Produced by Laser-assisted Technique. In *Nanodiamond*; Williams, O.; The Royal Society of Chemistry: Cambridge, 2014, pp 112−127.

(14) Khachatryan, A. K.; Aloyan, S. G.; May, P. W.; Sargsyan, R.; Khachatryan, V. A.; Baghdasaryan, V. S. Graphite-to-Diamond Transformation Induced by Ultrasound Cavitation. *Diamond Relat. Mater.* **2008**, *17* (6), 931−936.

(15) Kumar, A.; Ann Lin, P.; Xue, A.; Hao, B.; Khin Yap, Y.; Sankaran, R. M. Formation of Nanodiamonds at Near-Ambient Conditions via Microplasma Dissociation of Ethanol Vapour. *Nat. Commun.* **2013**, *4* (1), 2618.

(16) Lindner, S.; Bommer, A.; Muzha, A.; Krueger, A.; Gines, L.; Mandal, S.; Williams, O.; Londero, E.; Gali, A.; Becher, C. Strongly inhomogeneous distribution of spectral properties of silicon-vacancy color centers in nanodiamonds. *New Journal of Physics* **2018**, *20* (11), 115002.

(17) Abdullahi, I. M.; Langenderfer, M.; Shenderova, O.; Nunn, N.; Torelli, M. D.; Johnson, C. E.; Mochalin, V. N. Explosive Fragmentation of Luminescent Diamond Particles. *Carbon* **2020**, *164*, 442−450.

(18) Mochalin, V. N.; Gogotsi, Y. Nanodiamond−Polymer Composites. *Diamond Relat. Mater.* **2015**, *58*, 161−171.

(19) Turcheniuk, K.; Mochalin, V. N. Biomedical Applications of Nanodiamond (Review). *Nanotechnology* **2017**, *28* (25), 252001.

(20) Zhang, L.; Zhu, D.; Nathanson, G. M.; Hamers, R. J. Selective Photoelectrochemical Reduction of Aqueous CO_2 to CO by Solvated Electrons. *Angew. Chem.* **2014**, *126* (37), 9904−9908.

(21) Badziag, P.; Verwoerd, W. S.; Ellis, W. P.; Greiner, N. R. Nanometre-Sized Diamonds are More Stable than Graphite. *Nature* **1990**, *343* (6255), 244−245.

(22) Stein, S. E. Diamond and Graphite Precursors. *Nature* **1990**, *346* (6284), 517−517.

(23) Raty, J.-Y.; Galli, G.; Bostedt, C.; van Buuren, T. W.; Terminello, L. J. Quantum Confinement and Fullerenelike Surface Reconstructions in Nanodiamonds. *Phys. Rev. Lett.* **2003**, *90* (3), 037401.

(24) Gaebel, T.; Bradac, C.; Chen, J.; Say, J. M.; Brown, L.; Hemmer, P.; Rabeau, J. R. Size-Reduction of Nanodiamonds via Air Oxidation. *Diamond Relat. Mater.* **2012**, *21*, 28−32.

(25) Etzold, B. J. M.; Neitzel, I.; Kett, M.; Strobl, F.; Mochalin, V. N.; Gogotsi, Y. Layer-by-Layer Oxidation for Decreasing the Size of Detonation Nanodiamond. *Chem. Mater.* **2014**, *26* (11), 3479−3484.

(26) Stehlik, S.; Varga, M.; Ledinsky, M.; Miliaieva, D.; Kozak, H.; Skakalova, V.; Mangler, C.; Pennycook, T. J.; Meyer, J. C.; Kromka, A.; et al. High-Yield Fabrication and Properties of 1.4 nm Nanodiamonds with Narrow Size Distribution. *Sci. Rep.* **2016**, *6* (1), 38419.

(27) Sverjensky, D. A.; Huang, F. Diamond Formation Due to a pH Drop During Fluid−Rock Interactions. *Nat. Commun.* **2015**, *6* (1), 8702.

(28) Mansoori, G. A.; De Araujo, E. S.; De Araujo, P. L. B. *Diamondoid Molecules: With Applications In Biomedicine, Materials Science, Nanotechnology & Petroleum Science: With Applications in Biomedicine, Materials Science, Nanotechnology and Petroleum Science*; World Scientific Publishing Company: Singapore, 2012.

(29) Shen, Y.; Su, S.; Zhao, W.; Cheng, S.; Xu, T.; Yin, K.; Chen, L.; He, L.; Zhou, Y.; Bi, H.; et al. Sub-4 nm Nanodiamonds from Graphene-Oxide and Nitrated Polycyclic Aromatic Hydrocarbons at 423 K. *ACS Nano* **2021**, *15* (11), 17392−17400.

(30) Sudha, P. N.; Sangeetha, K.; Vijayalakshmi, K.; Barhoum, A. Nanomaterials History, Classification, Unique Properties, Production and Market. In *Emerging Applications of Nanoparticles and Architecture Nanostructures*; Barhoum, A., Makhlouf, A. S. H., Eds.; Elsevier, 2018; Chapter 12, pp 341−384.

(31) Kroto, H. W.; Heath, J. R.; O'Brien, S. C.; Curl, R. F.; Smalley, R. E. C60: Buckminsterfullerene. *Nature* **1985**, *318* (6042), 162−163.

(32) Erickson, H. P. Size and Shape of Protein Molecules at the Nanometer Level Determined by Sedimentation, Gel Filtration, and Electron Microscopy. *Biological Procedures Online* **2009**, *11* (1), 32.

(33) Koo, J.; Kim, I.; Kim, Y.; Cho, D.; Hwang, I.-C.; Mukhopadhyay, R. D.; Song, H.; Ko, Y. H.; Dhamija, A.; Lee, H.; et al. Gigantic Porphyrinic Cages. *Chem.* **2020**, *6* (12), 3374−3384.

(34) Font, F.; Myers, T. G. Spherically Symmetric Nanoparticle Melting with a Variable Phase Change Temperature. *J. Nanopart. Res.* **2013**, *15* (12), 2086.
(35) Navrotsky, A. Energetics at the Nanoscale: Impacts for Geochemistry, the Environment, and Materials. *MRS Bull.* **2016**, *41* (2), 139−145.
(36) Yu, J.; Yong, X.; Tang, Z.; Yang, B.; Lu, S. Theoretical Understanding of Structure−Property Relationships in Luminescence of Carbon Dots. *J. Phys. Chem. Lett.* **2021**, *12* (32), 7671−7687.
(37) Wilson, E. R.; Parker, L. M.; Orth, A.; Nunn, N.; Torelli, M.; Shenderova, O.; Gibson, B. C.; Reineck, P. The Effect of Particle Size on Nanodiamond Fluorescence and Colloidal Properties in Biological Media. *Nanotechnology* **2019**, *30* (38), 385704.
(38) Ishida, T.; Murayama, T.; Taketoshi, A.; Haruta, M. Importance of Size and Contact Structure of Gold Nanoparticles for the Genesis of Unique Catalytic Processes. *Chem. Rev.* **2020**, *120* (2), 464−525.
(39) Burdett, J. K. From Bonds to Bands and Molecules to Solids. *Prog. Solid State Chem.* **1984**, *15* (3), 173−255.
(40) Barnard, A. S. *The Diamond Formula: Diamond Synthesis: A Gemmological Perspective*; Butterworth-Heinemann: Oxford, 2000.
(41) Leypunskiy, O. I. Ob Iskusstvennikh Almazakh. *Usp. Khimii.* **1939**, No. 8, 1519−1534.
(42) Little, R.; Roache, J. Treatise on the Resolution of the Diamond Problem after 200 Years. *Prog. Solid State Chem.* **2008**, *36*, 223−251.
(43) Elshina, L. A.; Muradymov, R. V.; Elshin, A. N. Chemical Method of Producing Artificial Diamonds. Russia Patent Appl. 2586140 C1, 2015.
(44) Stehlik, S.; Varga, M.; Ledinsky, M.; Jirasek, V.; Artemenko, A.; Kozak, H.; Ondic, L.; Skakalova, V.; Argentero, G.; Pennycook, T.; et al. Size and Purity Control of HPHT Nanodiamonds Down to 1 nm. *J. Phys. Chem. C* **2015**, *119* (49), 27708−27720.
(45) Boudou, J.-P.; Tisler, J.; Reuter, R.; Thorel, A.; Curmi, P. A.; Jelezko, F.; Wrachtrup, J. Fluorescent Nanodiamonds Derived from HPHT with a Size of Less than 10nm. *Diamond Relat. Mater.* **2013**, *37*, 80−86.
(46) Kulakova, I. I. About Synthesis of Diamond. *Porodorazrush-ayuschiy i Metalloobrabatyvayuschiy Instrument - Tehnika i Tehnologiya Ego Izgotovleniya i Primeneniya (in Russian)* **2006**, No. 9, 179−185.
(47) Galimov, É. M.; Kudin, A. M.; Skorobogatskii, V. N.; Plotnichenko, V. G.; Bondarev, O. L.; Zarubin, B. G.; Strazdovskii, V. V.; Aronin, A. S.; Fisenko, A. V.; Bykov, I. V.; et al. Experimental Corroboration of the Synthesis of Diamond in the Cavitation Process. *Doklady Physics* **2004**, *49* (3), 150−153.
(48) Rudenko, A. P.; Kulakova, I. I.; Skvortsova, V. L. The Chemical Synthesis of Diamond. Aspects of the General Theory. *Russ. Chem. Rev.* **1993**, *62* (2), 87−104.
(49) Tzeng, Y.-K.; Zhang, J. L.; Lu, H.; Ishiwata, H.; Dahl, J.; Carlson, R. M. K.; Yan, H.; Schreiner, P. R.; Vučković, J.; Shen, Z.-X.; et al. Vertical-Substrate MPCVD Epitaxial Nanodiamond Growth. *Nano Lett.* **2017**, *17* (3), 1489−1495.
(50) Tiwari, R. N.; Tiwari, J. N.; Chang, L.; Yoshimura, M. Enhanced Nucleation and Growth of Diamond Film on Si by CVD Using a Chemical Precursor. *J. Phys. Chem. C* **2011**, *115* (32), 16063−16073.
(51) Ishiwata, H.; Shen, Z.-X.; Melosh, N. A.; Dahl, J. Diamond Growth Using Diamondoids. U.S. Patent Appl. 20130336873 A1, 2013.
(52) Gogotsi, Y.; Welz, S.; Ersoy, D. A.; McNallan, M. J. Conversion of Silicon Carbide to Crystalline Diamond-Structured Carbon at Ambient Pressure. *Nature* **2001**, *411* (6835), 283−287.
(53) Guo, B.; Wu, W.; Ma, H.; Zhang, Z.; Zhang, Z.; Gao, W.; Zhou, W.; Zhang, R. Catalytic Synthesis of Nanodiamond Based on CDC Principle: Influence of Different Catalysts on Types and Sizes. *Nanotechnology* **2021**, *32* (39), 395604.
(54) Prawer, S.; Nemanich, R. J. Raman Spectroscopy of Diamond and Doped Diamond. *Philosophical Transactions: Mathematical, Physical and Engineering Sciences* **2004**, *362* (1824), 2537−2565.
(55) Sabitov, S.; Mansurov, B.; Medyanova, B.; Partizan, G.; Koshanova, A.; Merkibayev, Y.; Mansurova, M.; Lesbayev, B. Synthesis of Micro- and Nanodiamonds by the Method of Oxy-Acetylene Combustion Flame. *Journal of Physics: Conference Series* **2016**, *741*, 012023.
(56) Su, Z.; Zhou, W.; Zhang, Y. New Insight into the Soot Nanoparticles in a Candle Flame. *Chem. Commun.* **2011**, *47* (16), 4700−4702.
(57) Zhang, J.; Feng, Y.; Ishiwata, H.; Miyata, Y.; Kitaura, R.; Dahl, J. E. P.; Carlson, R. M. K.; Shinohara, H.; Tománek, D. Synthesis and Transformation of Linear Adamantane Assemblies inside Carbon Nanotubes. *ACS Nano* **2012**, *6* (10), 8674−8683.
(58) Ender, C. P.; Liang, J.; Friebel, J.; Zapata, T.; Wagner, M.; Ermakova, A.; Weil, T. Mechanistic Insights of Seeded Diamond Growth from Molecular Precursors. *ChemRxiv* **2021**; https://chemrxiv.org/engage/chemrxiv/article-details/6103a1f8880443ac59e48736 (accessed 2022-02-23).
(59) Kawamura, H.; Ohfuji, H. Nano-Polycrystalline Diamond Synthesized through the Decomposition of Stearic Acid. *High Pressure Research* **2020**, *40* (1), 162−174.
(60) Li, Y.; Qian, Y.; Liao, H.; Ding, Y.; Yang, L.; Xu, C.; Li, F.; Zhou, G. A Reduction-Pyrolysis-Catalysis Synthesis of Diamond. *Science* **1998**, *281* (5374), 246−247.
(61) Lou, Z.; Chen, Q.; Zhang, Y.; Wang, W.; Qian, Y. Diamond Formation by Reduction of Carbon Dioxide at Low Temperatures. *J. Am. Chem. Soc.* **2003**, *125* (31), 9302−9303.
(62) Kamali, A. R. Nanocatalytic Conversion of CO2 into Nanodiamonds. *Carbon* **2017**, *123*, 205−215.
(63) Petit, T.; Arnault, J.-C.; Girard, H. A.; Sennour, M.; Bergonzo, P. Early Stages of Surface Graphitization on Nanodiamond Probed by X-Ray Photoelectron Spectroscopy. *Phys. Rev. B* **2011**, *84* (23), 233407.
(64) Mermoux, M.; Chang, S.; Girard, H. A.; Arnault, J.-C. Raman Spectroscopy Study of Detonation Nanodiamond. *Diamond Relat. Mater.* **2018**, *87*, 248−260.
(65) Mermoux, M. Raman Investigations on Nanodiamonds. In *Nanodiamonds*; Arnault, J.-C., Ed.; Elsevier: Amsterdam, 2017; Chapter 4, pp 85−107.
(66) Korepanov, V. I.; Hamaguchi, H.; Osawa, E.; Ermolenkov, V.; Lednev, I. K.; Etzold, B. J. M.; Levinson, O.; Zousman, B.; Epperla, C. P.; Chang, H.-C. Carbon Structure in Nanodiamonds Elucidated from Raman Spectroscopy. *Carbon* **2017**, *121*, 322−329.
(67) Mochalin, V.; Osswald, S.; Gogotsi, Y. Contribution of Functional Groups to the Raman Spectrum of Nanodiamond Powders. *Chem. Mater.* **2009**, *21* (2), 273−279.
(68) Shiell, T. B.; McCulloch, D. G.; Bradby, J. E.; Haberl, B.; Boehler, R.; McKenzie, D. R. Nanocrystalline Hexagonal Diamond Formed from Glassy Carbon. *Sci. Rep.* **2016**, *6* (1), 37232.
(69) Chang, S. L. Y.; Dwyer, C.; Ōsawa, E.; Barnard, A. S. Size Dependent Surface Reconstruction in Detonation Nanodiamonds. *Nanoscale Horizons* **2018**, *3* (2), 213−217.
(70) Barnard, A. S.; Russo, S. P.; Snook, I. K. Coexistence of Bucky Diamond with Nanodiamond and Fullerene Carbon Phases. *Phys. Rev. B* **2003**, *68* (7), 073406.
(71) Garvie, L. A. J.; Buseck, P. R. Carbonaceous Materials in the Acid Residue from the Orgueil Carbonaceous Chondrite Meteorite. *Meteoritics & Planetary Science* **2006**, *41* (4), 633−642.
(72) Chang, S. L. Y.; Barnard, A. S.; Dwyer, C.; Boothroyd, C. B.; Hocking, R. K.; Ōsawa, E.; Nicholls, R. J. Counting Vacancies and Nitrogen-Vacancy Centers in Detonation Nanodiamond. *Nanoscale* **2016**, *8* (20), 10548−10552.
(73) Braun, A.; Kubatova, A.; Wirick, S.; Mun, S. B. Radiation Damage from EELS and NEXAFS in Diesel Soot and Diesel Soot Extracts. *J. Electron Spectrosc. Relat. Phenom.* **2009**, *170* (1), 42−48. D'Angelo, D.; Bongiorno, C.; Amato, M.; Deretzis, I.; La Magna, A.; Fazio, E.; Scalese, S. Oxygen Functionalities Evolution in Thermally Treated Graphene Oxide Featured by EELS and DFT Calculations. *J. Phys. Chem. C* **2017**, *121* (9), 5408−5414.
(74) D'Angelo, D.; Bongiorno, C.; Amato, M.; Deretzis, I.; La Magna, A.; Fazio, E.; Scalese, S. Oxygen Functionalities Evolution in Thermally Treated Graphene Oxide Featured by EELS and DFT Calculations. *J. Phys. Chem. C* **2017**, *121* (9), 5408−5414.

https://doi.org/10.1021/acsnano.2c00197
ACS Nano 2022, 16, 8513−8524

(75) Wang, C.; Zheng, B.; Zheng, W. T.; Jiang, Q. Electronic Properties of Dehydrogenated Nanodiamonds: A First-Principles Study. *Diamond Relat. Mater.* **2008**, *17* (2), 204−208.
(76) Willey, T. M.; Bostedt, C.; van Buuren, T.; Dahl, J. E.; Liu, S. G.; Carlson, R. M. K.; Terminello, L. J.; Möller, T. Molecular Limits to the Quantum Confinement Model in Diamond Clusters. *Phys. Rev. Lett.* **2005**, *95* (11), 113401.
(77) Hoffman, A.; Laikhtman, A. Photon Stimulated Desorption of Hydrogen from Diamond Surfaces via Core-Level Excitations: Fundamental Processes and Applications to Surface Studies. *J. Phys.: Condens. Matter* **2006**, *18* (30), S1517−S1546.
(78) Hitchcock, A. P.; Horsley, J. A.; Stöhr, J. Inner Shell Excitation of Thiophene and Thiolane: Gas, Solid, and Monolayer States. *J. Chem. Phys.* **1986**, *85* (9), 4835−4848.
(79) Hiraki, J.; Mori, H.; Taguchi, E.; Yasuda, H.; Kinoshita, H.; Ohmae, N. Transformation of Diamond Nanoparticles into Onion-Like Carbon by Electron Irradiation Studied Directly Inside an Ultrahigh-Vacuum Transmission Electron Microscope. *Appl. Phys. Lett.* **2005**, *86* (22), 223101.
(80) Perevedentseva, E.; Lin, Y.-C.; Cheng, C.-L. A Review of Recent Advances in Nanodiamond-Mediated Drug Delivery in Cancer. *Expert Opinion on Drug Delivery* **2021**, *18* (3), 369−382.
(81) Gao, G.; Guo, Q.; Zhi, J. Nanodiamond-Based Theranostic Platform for Drug Delivery and Bioimaging. *Small* **2019**, *15* (48), 1902238.
(82) Haziza, S.; Mohan, N.; Loe-Mie, Y.; Lepagnol-Bestel, A.-M.; Massou, S.; Adam, M.-P.; Le, X. L.; Viard, J.; Plancon, C.; Daudin, R.; et al. Fluorescent Nanodiamond Tracking Reveals Intraneuronal Transport Abnormalities Induced by Brain-Disease-Related Genetic Risk Factors. *Nat. Nanotechnol.* **2017**, *12* (4), 322−328.
(83) Reineck, P.; Lau, D. W. M.; Wilson, E. R.; Fox, K.; Field, M. R.; Deeleepojananan, C.; Mochalin, V. N.; Gibson, B. C. Effect of Surface Chemistry on the Fluorescence of Detonation Nanodiamonds. *ACS Nano* **2017**, *11* (11), 10924−10934.
(84) Zaitsev, A. M. *Optical Properties of Diamond: a Data Handbook*; Springer Science & Business Media: Berlin, 2013.
(85) Dei Cas, L.; Zeldin, S.; Nunn, N.; Torelli, M.; Shames, A. I.; Zaitsev, A. M.; Shenderova, O. From Fancy Blue to Red: Controlled Production of a Vibrant Color Spectrum of Fluorescent Diamond Particles. *Adv. Funct. Mater.* **2019**, *29* (19), 1808362.
(86) De Feudis, M.; Tallaire, A.; Nicolas, L.; Brinza, O.; Goldner, P.; Hétet, G.; Bénédic, F.; Achard, J. Large-Scale Fabrication of Highly Emissive Nanodiamonds by Chemical Vapor Deposition with Controlled Doping by SiV and GeV Centers from a Solid Source. *Advanced Materials Interfaces* **2020**, *7* (2), 1901408.
(87) Shames, A. I.; Dalis, A.; Greentree, A. D.; Gibson, B. C.; Abe, H.; Ohshima, T.; Shenderova, O.; Zaitsev, A.; Reineck, P. Near-Infrared Fluorescence from Silicon- and Nickel-Based Color Centers in High-Pressure High-Temperature Diamond Micro- and Nanoparticles. *Advanced Optical Materials* **2020**, *8* (23), 2001047.
(88) Shenderova, O.; Nunn, N.; Oeckinghaus, T.; Torelli, M.; McGuire, G.; Smith, K.; Danilov, E.; Reuter, R.; Wrachtrup, J.; Shames, A.; et al. Commercial Quantities of Ultrasmall Fluorescent Nanodiamonds Containing Color Centers. *Proc.SPIE* **2017**, 1011803.
(89) Vlasov, I. I.; Shiryaev, A. A.; Rendler, T.; Steinert, S.; Lee, S.-Y.; Antonov, D.; Vörös, M.; Jelezko, F.; Fisenko, A. V.; Semjonova, L. F.; et al. Molecular-Sized Fluorescent Nanodiamonds. *Nat. Nanotechnol.* **2014**, *9* (1), 54−58.
(90) Bradac, C.; Gaebel, T.; Naidoo, N.; Sellars, M. J.; Twamley, J.; Brown, L. J.; Barnard, A. S.; Plakhotnik, T.; Zvyagin, A. V.; Rabeau, J. R. Observation and Control of Blinking Nitrogen-Vacancy Centres in Discrete Nanodiamonds. *Nat. Nanotechnol.* **2010**, *5* (5), 345−349.
(91) Petrone, A.; Goings, J. J.; Li, X. Quantum Confinement Effects on Optical Transitions in Nanodiamonds Containing Nitrogen Vacancies. *Phys. Rev. B* **2016**, *94* (16), 165402.
(92) Wang, Z.-H.; Takahashi, S. Spin Decoherence and Electron Spin Bath Noise of a Nitrogen-Vacancy Center in Diamond. *Phys. Rev. B* **2013**, *87* (11), 115122.
(93) Capelli, M.; Lindner, L.; Luo, T.; Jeske, J.; Abe, H.; Onoda, S.; Ohshima, T.; Johnson, B.; Simpson, D. A.; Stacey, A.; et al. Proximal Nitrogen Reduces the Fluorescence Quantum Yield of Nitrogen-Vacancy Centres in Diamond. *New J. Phys.* **2022**, *24* (3), 033053.
(94) Zhang, T.; Pramanik, G.; Zhang, K.; Gulka, M.; Wang, L.; Jing, J.; Xu, F.; Li, Z.; Wei, Q.; Cigler, P.; et al. Toward Quantitative Bio-sensing with Nitrogen−Vacancy Center in Diamond. *ACS Sensors* **2021**, *6* (6), 2077−2107.
(95) Tisler, J.; Balasubramanian, G.; Naydenov, B.; Kolesov, R.; Grotz, B.; Reuter, R.; Boudou, J.-P.; Curmi, P. A.; Sennour, M.; Thorel, A.; et al. Fluorescence and Spin Properties of Defects in Single Digit Nanodiamonds. *ACS Nano* **2009**, *3* (7), 1959−1965.
(96) Kaviani, M.; Deák, P.; Aradi, B.; Frauenheim, T.; Chou, J.-P.; Gali, A. Proper Surface Termination for Luminescent Near-Surface NV Centers in Diamond. *Nano Lett.* **2014**, *14* (8), 4772−4777. Karim, A.; Lyskov, I.; Russo, S. P.; Peruzzo, A. An ab initio effective solid-state photoluminescence by frequency constraint of cluster calculation. *J. Appl. Phys.* **2020**, *128* (23), 233102.
(97) Karim, A.; Lyskov, I.; Russo, S. P.; Peruzzo, A. An ab initio effective solid-state photoluminescence by frequency constraint of cluster calculation. *Journal of Applied Physics* **2020**, *128* (23), 233102.
(98) Worboys, J. G.; Drumm, D. W.; Greentree, A. D. Quantum Multilateration: Subdiffraction Emitter Pair Localization via Three Spatially Separate Hanbury Brown and Twiss Measurements. *Phys. Rev. A* **2020**, *101* (1), 013810.
(99) Zapata, T.; Bennett, N. R.; Struzhkin, V. V.; Fei, Y.; Jelezko, F.; Biskupek, J.; Kaiser, U.; Reuter, R.; Wrachtrup, J.; Ghannam, F. A.; et al. Organic Nanodiamonds. *arXiv* **2017**; https://arxiv.org/abs/1702.06854 (accessed 2022-04-20).

https://doi.org/10.1021/acsnano.2c00197
ACS Nano 2022, 16, 8513−8524